Correlation Analysis of Atomic and Single-Molecule Junction Conductance

Péter Makk,[†] Damian Tomaszewski,[‡] Jan Martinek,[‡] Zoltán Balogh,[†] Szabolcs Csonka,[†] Maciej Wawrzyniak,[¶] Michael Frei,[§] Latha Venkataraman,[§,*] and András Halbritter[†,*]

[†]Department of Physics, Budapest University of Technology and Economics and Condensed Matter Research Group of the Hungarian Academy of Sciences, 1111 Budapest, Budafoki ut 8., Hungary, [‡]Institute of Molecular Physics, Polish Academy of Sciences, 60-179 Poznań, Poland, [¶]Faculty of Electronics and Telecommunications, Poznań University of Technology, Poznań, Poland, and [§]Department of Applied Physics and Applied Mathematics, Columbia University, New York, New York 10027, United States

The break-junction technique is widely used to create atomic-scale nanowires, in which the current is flowing through a single or a few atoms or molecules.[1,2] The basic idea of the technique is the controlled mechanical elongation of a metallic nanowire. Before rupture, the cross section of the wire narrows to atomic dimensions giving a unique possibility to study the electron transport through single or a few atoms connecting two metallic electrodes.[1] The break junction technique has recently been applied in the field of molecular electronics to measure transport characteristics of single-molecule junctions,[3−8] as the atomic-scale, variable width gap formed after breaking a single-atom contact provides an ideal platform for contacting single molecules.

The precise atomic structure of the junction, however, is not well controlled in the measurement, which is reflected by a stochastic behavior of the experimental observables from junction to junction. To record the features which are typical and universal for a broad variety of independently created junctions a statistical analysis is required. Typically, conductance is recorded as a function of electrode separation during the rupture of a particular nanowire, yielding *conductance traces*. Such traces can be measured several times by repeatedly closing and opening the junction. After recording thousands of independent conductance traces a conductance histogram can be created, in which peaks may be observed reflecting the conductance of stable, frequently occurring junction configurations.[1] For nanoscale junctions of pure metals the conductance peak with the smallest value usually corresponds to the conductance of a single-atom contact. When metal contacts are broken in an environment of molecules, new conductance peaks may be seen in the

ABSTRACT
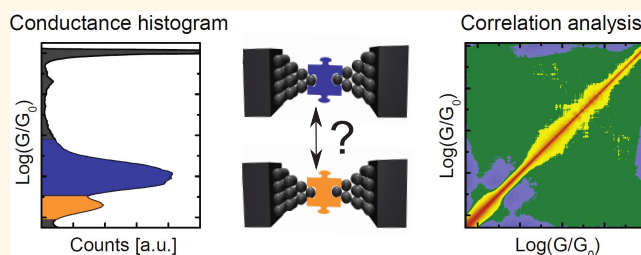
The break-junction technique is widely used to measure electronic properties of nanoscale junctions including metal point-contacts and single-molecule junctions. In these measurements, conductance is measured as a function of electrode displacement yielding data that is analyzed by constructing conductance histograms to determine the most frequently observed conductance values in the nanoscale junctions. However much of the rich physics in these measurements is lost in this simple analysis technique. Conductance histograms cannot be used to study the statistical relation of distinct junction configurations, to distinguish structurally different configurations that have similar conductance values, or to obtain information on the relation between conductance and junction elongation. Here, we give a detailed introduction to a novel statistical analysis method based on the two-dimensional cross-correlation histogram (2DCH) analysis of conductance traces and show that this method provides new information about the relation of different junction configurations that occur during the formation and evolution of metal and single-molecule junctions. We first illustrate the different types of correlation effects by using simulated conductance traces. We then apply this analysis method to several different experimental examples. We show from break-junction measurements of different metal point-contacts that in aluminum, the first conductance histogram peak corresponds to two different junction structures. In tantalum, we identify the frequent absence of adhesive instability. We show that conductance plateaus shift in a correlated manner in iron and vanadium junctions. Finally, we highlight the applicability of the correlation analysis to single-molecule platinum—CO—platinum and gold—4,4′-bipyridine—gold junctions.

histogram, which result from the formation of stable molecular configurations that have similar conductances.[3−8]

Despite their broad application, conductance histograms provide limited information about the system under study. The histogram is considered as a mean value indicating the presence of distinct junction configurations with the same conductance

values. However, to obtain information about the *relation* between these configurations one has to go beyond histograms. Several attempts have been made to extract additional information from the measured conductance traces, which is not resolved by the conductance histogram. A demonstrative example was the plateaus' length analysis introduced by A. I. Yanson and co-workers, which gave clear evidence for the formation of monatomic chains in Au, Pt, and Ir nanoscale junctions.[9,10] In recent break junction measurements on single molecule junctions a two-dimensional analysis method was introduced to relate junction conductance to electrode displacement in a statistical manner.[8,11−16]

More recently, a novel cross correlation analysis of the conductance traces was shown to provide a more detailed understanding of atomic junctions.[13,17] Correlation analysis is inspired by the 2D correlation spectroscopy in magnetic resonances[18] as well as by analysis of noise measurements,[19] where the correlated deviation from the mean value is an important indicator of fundamental properties such as the bosonic or fermionic nature of the particles under study,[20−22] or the absence or presence of quantum entangled particle pairs.[23] In break-junction based conductance measurements, correlation analysis can be used to resolve several features of junction formation and evolution which are hidden in traditional conductance histograms. One example is when a molecule binds in two different configurations which have different conductances in a correlated way where the formation of one configuration may either assist or hamper the formation of the other one. Two peaks in conductance histogram reflect the occurrence of both configurations in the data, but a correlation analysis is required to understand the relation between these configurations. Furthermore, if the conductance of a junction evolves upon elongation in different ways depending on the structural details of its contacts at the atomic scale, a wide histogram peak could result. A cross-correlation analysis of the data could then be used to differentiate various junction evolution trajectories.[13]

In this work, we describe in detail the correlation analysis method and apply it on different break-junction based conductance measurements. We show how two-dimensional cross-correlation histograms (2DCH) are generated starting with conductance traces and then show how to interpret different features in these 2DCH, to resolve aspects of junction formation and evolution that are not seen in standard conductance histograms. First different analysis methods are described that can be applied to conductance data. This is followed by the illustration of these analysis methods on simulated conductance traces. Finally we apply these analysis techniques to different experimental data sets including measurements of metal point-contacts and single-molecule junctions.

RESULTS AND DISCUSSION

Analysis Techniques for Conductance Measurements. In the experiments, conductance is measured as a function of junction elongation to yield conductance traces which show the evolution of the conductance as the nanoscale junction is ruptured. During the final stage of rupture, conductance typically decreases stepwise as the electrodes are pulled apart. This results in conductance traces having plateaus separated by sharp drops, as shown in Figure 1a for the rupture of Al point-contacts. The plateaus correspond to elastic stretching of stable atomic configurations; the jumps result from atomic rearrangements between different configurations.[1] After rupture the contact can be closed again, and the rupture can be repeated several thousand times. Since each trace corresponds to the conductance evolution of a different junction, large trace-to-trace variations exist due to the stochastic nature of contact formation dynamics. Therefore, any reliable experimental statement must be based on the analysis of a statistical ensemble of conductance traces containing several thousand individual measurements.

In this section we define and describe different analysis methods that can be applied to conductance data. We start with one-dimensional conductance histograms which are used to determine the most frequently occurring conductance values in a break-junction experiment. We briefly review the constructions of two-dimensional conductance-displacement histograms,[11,12] which provide information on the elongation length of structures with the same conductance values. Finally we describe the correlation analysis method and show how to construct two-dimensional correlation histograms (2DCH) and conditional histograms.

Conductance Histograms. A conductance histogram is constructed by dividing the conductance axis to discrete bins of width δ_G labeled by i so that the conductance of a bin G_i is given by $G_i = (i - 1/2) \cdot \delta_G$. For each trace r, the number of data points N in each conductance bin is determined. $N_i(r)$ is then the conductance histograms for the rth individual trace, as demonstrated in Figure 1b. With this notation the conductance histogram for the whole data set is obtained by averaging the individual histogram from all traces:

$$H_i = \langle N_i(r) \rangle_r = \frac{1}{R} \sum_{r=1}^{R} N_i(r) \tag{1}$$

Here, R is the total number of traces included in the analysis (Figure 1c). For atomic scale structures the conductance axis of the histogram is usually plotted in units of the conductance quantum, $G_0 = 2e^2/h$, and the bin width used ranges from 0.01 to 0.05 G_0. The above
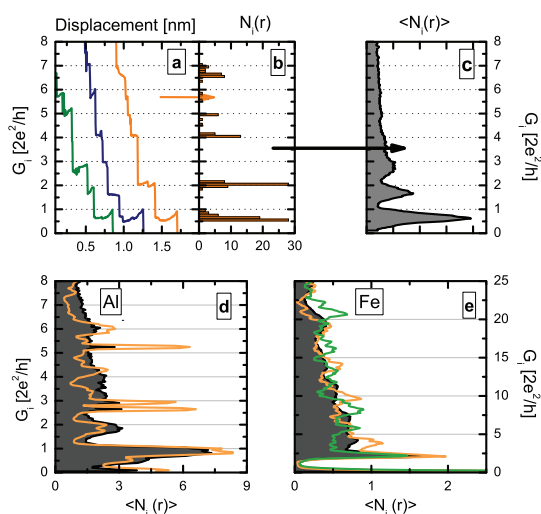
Figure 1. (a) Representative conductance traces for Al junctions showing plateaus separated by conductance jumps. (b) Conductance histogram for the orange conductance trace from panel a. (c) Conductance histogram $\langle N_i(r)\rangle_r$ for the whole data set of 5000 conductance traces. (d) Conductance histogram for another Al data set of 5000 traces (gray area graph) and a subset histogram for 100 consecutive traces which differ considerably. (d) Histogram for an Fe data set of 5000 traces (gray) together with the subset histograms (orange and green) for the first and final 100 traces, respectively.

definition demonstrates that the conductance histograms represent the mean value of a stochastic quantity, $N_i(r)$.

In a reliable and statistically diverse data set, the total conductance histogram, H_i does not vary with time. To ensure that a given data set is reliable, it is useful to check that the conductance histograms for different subsets of the data (typically including 100−200 consecutive traces) coincide with the total histogram.

In Figure 1d, we show a conductance histogram for another Al data set constructed from 5000 traces (gray area graph) and a conductance histogram for a particular subset including only 100 traces. In contrast to the total histogram the subset histogram (orange line) exhibits sharp peaks, indicating that a diverse set of junctions is not measured but rather measurements of a single junction structure are repeated multiple times.[24] This can result in low temperature measurements if the contact is not pushed together enough to form a junction with a conductance larger than than $\sim$40 G_0 (for most metals, or $\sim$10 G_0 for gold) before it is elongated and ruptured.

Figure 1e shows an example for Fe junctions where the subset histogram for the final 100 traces (green curve) shows a significant variation of the structures compared to the initial 100 traces (orange curve), which yields a smearing of the peaks in the total histogram (gray area graph). Such variation may occur in the majority of the metals due to a temporal

variation of the junction structures, like the slow fluctuation of the dominant crystallographic orientation of the junction. Although such temporal variation of the conductance histogram occurs in long measurements, different segments of such large data sets can be analyzed separately.

The correlation analysis presented below is especially sensitive to the temporal homogeneity of the data, therefore it is essential to exclude data which show a significant temporal variation.

Two-Dimensional Conductance-Displacement Histograms. Conductance histograms described above do not retain any displacement information. A statistical analysis including displacement information can be obtained by constructing a two-dimensional conductance-displacement histogram as demonstrated by Quek et al.[11] and Martin et al.[12] This is carried out as follows: each conductance trace represents conductance (G) as a function of displacement (x), thus each rth trace can be written as the function $G_r(x)$. However, the absolute electrode position (x) has no physical meaning. To compare different conductance traces, each curve must be shifted along the electrode separation axis to a common physical origin with the same conductance value. Thus every measured trace is offset by a distance x_r such that $G_r(x − x_r) = G_{ref}$ as shown in Figure 2b for measurements of Pt metal point contact. Two-dimensional conductance-displacements histograms can then be created by summing all the offset traces using conductance along the vertical axis and relative displacement along the horizontal axis. This is achieved by dividing each axis into discrete two-dimensional bins and summing the number of data points in each bin from all offset traces. In single molecule conductance measurements the reference conductance, G_{ref} is usually set at a conductance smaller than that of the single-atom conductance ($\sim$1 G_0) but larger than that of the molecular conductance. In typical measurements,[11] G_{ref} is set to 0.5 G_0. Since the weight in the conductance histogram at G_{ref} is small, the 2D histogram is not sensitive to its exact value.

Figure 2c shows a 2D conductance-displacement histogram of Pt metal point contacts, where the solid vertical line shows the new common origin. To study the nature of the final plateaus before rupture the reference conductance, G_{ref} is set to the conductance value at minimum between the first and second peak in the conductance histogram of platinum (Figure 2a), G_{ref} = 2.5 G_0. The 2D histogram in Figure 2c shows that the length of the last plateau ($\sim$0.6 nm) is considerably longer than the interatomic distance, and the weight in the tunneling region is modulated with a period of the interatomic distance ($\sim$0.25 nm). This is consistent with the notion that the Pt single-atom contact ruptures after forming a monatomic chain with different numbers of atoms as has been seen before.[10]
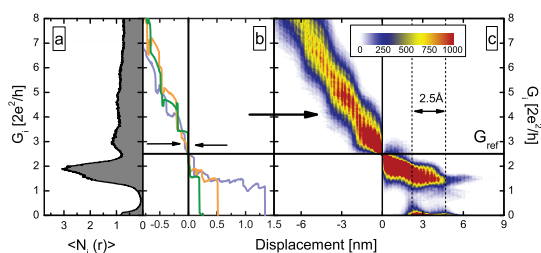
Figure 2. The construction of 2D conductance-displacement histograms demonstrated by a data set of pure Pt junctions measured at $T = 4.2$ K. Panels a, b, and c show the conductance histogram, examples traces, and conductance-displacement histogram. Dashed lines in panel c represent the displacement where there is an increased weight in conductance region below 0.3 G_0. These correspond to the most likely location of junction rupture.

Two-Dimensional Cross-Correlation Histograms. Conductance histograms study the relative occurrence of junction configurations at *single* conductance values. The 2D conductance-displacement histograms show the relative occurrence of a conductance value at a certain electrode separation relative to a fixed conductance value. To determine the statistical relation between two different junction configurations that correspond to two particular conductance values, a correlation analysis needs to be carried out. In this section we introduce several types of correlation functions that can provide different complementary information about the presence of correlations in conductance data.

The statistical relation of two configurations with conductances G_i and G_j in an individual trace can be determined from the product $N_i(r) \cdot N_j(r)$. By averaging this product for all traces, we can define the *2D cross-product histogram*[17] as

$$H_{i,j}^{cross} = \langle N_i(r) \cdot N_j(r) \rangle_r \tag{2}$$

In a given trace, if the number of data points in bin i is statistically independent from the number of data points in bin $j(\neq i)$, then $\langle N_i(r) \cdot N_j(r) \rangle_r$ factorizes to $\langle N_i(r) \rangle_r \cdot \langle N_j(r) \rangle_r$; that is, $H_{i,j}^{cross} = H_i \cdot H_j$. Figure 3a shows a 2D cross-product histogram for conductance data measured from Al point-contacts. The vertical and horizontal axes represent the conductance values G_i and G_j, and the color scale represents $H_{i,j}^{cross}$. In comparison the 2D simple product histogram ($H_i \cdot H_j$) is shown in Figure 3b. We see some clear differences between these two figures in the conductance range of the first histogram peak (0.15−1 G_0). The difference between these two figures (except for the trivial difference at the diagonal) shows regions where the corresponding number of data points in a pair of bins are not statistically independent from each other.

To detect minor correlations it is easier to study the difference of the cross-product histogram and the

product of the normal histograms, which we call *2D covariance histogram*:

$$H_{i,j}^{cov} = \langle N_i(r) \cdot N_j(r) \rangle_r - \langle N_i(r) \rangle_r \cdot \langle N_j(r) \rangle_r$$

$$= \langle \delta N_i(r) \cdot \delta N_j(r) \rangle_r. \tag{3}$$

Here, $\delta N_{i/j}(r) = N_{i/j}(r) - \langle N_{i/j}(r) \rangle$ denote the deviation from the mean values. The covariance, as defined above, is exactly zero if $N_i(r)$ and $N_j(r)$ are independent from each other. If the occurrence of two plateaus near bins i and j is correlated, that is, either both of them or neither of them appear in an individual trace, then both $N_i(r)$ and $N_j(r)$ will be larger or smaller, respectively, than their average values, yielding a positive covariance. In contrast, if the two plateaus are anticorrelated such that having a plateau near bin i excludes a plateau at bin j (or vice versa), the product $\delta N_i(r) \cdot \delta N_j(r)$ will be negative. In Figure 3c we show the 2D covariance histogram constructed from the same traces used to create Figure 3a. In this panel, to highlight the sign of the correlation a special color scale is used with positively correlated regions shown in shades of yellow/red, the negatively correlated regions shown in shades of blue/black, and uncorrelated regions shown in green.

The numerical value of the covariance histogram is not well-defined. If the normal histogram, H_i is uniformly rescaled (*e.g.*, the sampling rate is changed in the measurement) the covariance histogram will also be rescaled. Furthermore, the covariance histogram highlights the correlation effects in regions where either H_i or H_j (or both) exhibit peaks, and suppresses correlation effects where the weight of the conductance histogram is low. The covariance histogram therefore convolves histogram structure with correlation effects.

A proper normalization of the covariance histogram can be achieved using the standard definition of the correlation function:

$$H_{i,j}^{corr} = \frac{\langle \delta N_i(r) \cdot \delta N_j(r) \rangle_r}{\sqrt{\langle [\delta N_i(r)]^2 \rangle_r \langle [\delta N_j(r)]^2 \rangle_r}} \tag{4}$$

The *2D correlation histogram* created in such a way has well-defined limits: $-1 \leq C_{i,j}^{corr} \leq 1$. The correlation function is symmetric, $H_{i,j}^{cross} = H_{i,j}^{cross}$, and the diagonal is always unity, $H_{i,j}^{cross} = 1$. Furthermore, the scale of the correlation is not suppressed due to the low counts in the normal histogram. We show, in Figure 3d the 2D cross-correlation histogram for the same Al data set, which resolves additional features in the region ($G > 2$ G_0), where the 2D covariance histogram is suppressed due to the low weight of the conductance histogram.

Conditional Histograms. In general, data analysis is carried out using all measured traces. However, it can be useful to analyze a subset of the data, for example,
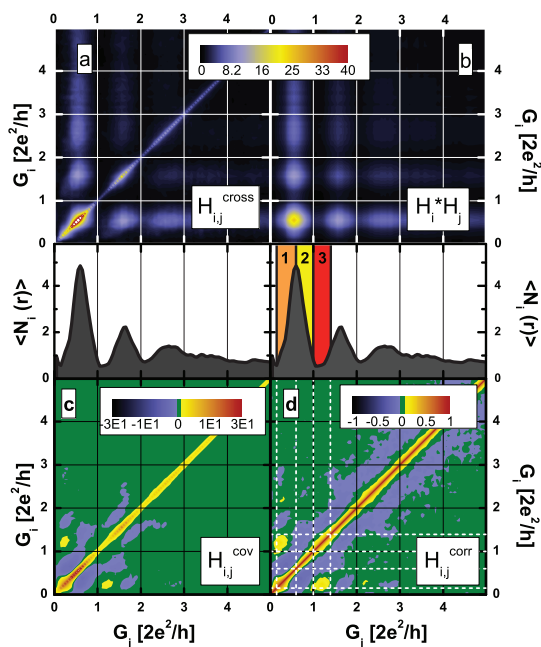
Figure 3. Correlation analysis of the same Al data set presented in Figure 1a—c. (a) 2D cross-product histogram, $H_{i,j}^{cross}$. (b) Product of the conductance histograms, $H_i \cdot H_j$. (c) 2D covariance histogram, $H_{i,j}^{cov}$. (d) 2D correlation histogram, $H_{i,j}^{corr}$. The middle panels show the conductance histogram. In the histogram on the right, the colored regions mark the first, second, and third conductance regions, respectively, as defined in the text. The white dashed lines in panel d delineate these conductance regions.

by selecting traces that give a major contribution to a certain histogram peak.[25] Histograms generated from a selected subset (conditional histograms) can provide information on the correlation between different junctions structures. If two histogram peaks correspond to statistically correlated (uncorrelated) atomic configurations, then the selection of the traces for one peak will (will not) change the second peak.

The selection of traces from a complete data set is performed by a simple algorithm: the traces r' for which the total number of data points in the interval of the reference histogram peak (P) is larger than a threshold value, N_P are selected.

$$H_i^{cond}(P) = \langle N_i(r') \rangle_{r'} \quad (5)$$

where traces r' are chosen using the condition

$$\sum_{j \in P} N_j(r') > N_P \quad (6)$$

The threshold value is usually defined as the average number of data points in the conductance region as

$$N_P = \left\langle \sum_{j \in P} N_j(r) \right\rangle_r \quad (7)$$

where the averaging is performed for all the traces. Both the total histogram, H_i and the conditional

histogram, H_i^{cond} are normalized to the number of traces included, so they can be compared directly, and their difference can point to the presence of correlations. In general, a conditional histogram is created to look for correlations in the occurrence of structures corresponding to different characteristic regions of the histogram. If the conductance histogram of the full data set does not show clear structures, then such an analysis is less reasonable.

This conditional histogram technique can be generalized to a 2D correlation method by replacing the peak interval P by a single conductance bin j, that is, constructing the conditional histogram from those traces that give a larger than average contribution to the bin j, $H_{i,j}^{cond}$. The difference between this conditional histogram and the total histogram, $H_{i,j}^{cond} - H_i$ can be visualized as a 2D color plot, and generally shows a structure similar to that of the 2D correlation histogram, and so it provides an alternative interpretation of correlation effects on the language of conductance histograms.

Throughout this paper we will use the 2DCH to analyze data from different experiments and supplement this with conditional histograms defined by eqs 5,—7.

Simulation of Correlation Histograms for Example Traces. The correlation histograms are able to show several features which are hidden in conductance histograms; however, their interpretation is not straightforward. Before applying this technique to actual data, we will illustrate, in this section, different types of features in these histograms using simulated traces with different character. This is carried out by generating single-trace conductance histograms $N_i(r)$ using a random number generator that follows some basic rules to reproduce different types of conductance traces.

Traces with a Single Conductance Plateau. We first consider traces with a single flat conductance plateau with unit length at a conductance $\mathscr{G}$ with a Gaussian distribution (mean of $\bar{\mathscr{G}}$ and a standard deviation of $\sigma = 0.08\bar{\mathscr{G}}$) as shown in Figure 4a. (Note that throughout this section the conductances are integer numbers coinciding with the corresponding bin label.) Experimentally nearly flat conductance plateaus are frequently seen on the conductance traces of noble metals,[1] with minor corrections due to conductance fluctuations.[26] We generate histograms of such traces with an added background noise $\mathscr{B}(i,r)$ to each bin to ensure that the denominator of the correlation function ($H_{i,j}^{corr}$) is finite. The background is a uniformly distributed random variable ranging from 0 to $\mathscr{B}_{max}$. Each single-trace conductance histogram is therefore defined as

$$N_i(r) = \delta_{i,\mathscr{G}(r)} + \mathscr{B}(i,r) \quad (8)$$

where δ is a Kronecker delta.

In Figure 4b and Figure 4c, we show the 2DCH and conductance histogram created from 20000 simulated traces. We see a perfectly correlated region ($H_{i,i}^{corr} = 1$) along the diagonal. In the conductance range spanning the width of the histogram peak, we see a negatively correlated region. This is a natural consequence of having a single flat plateau of unit length in the traces. If a trace r has a plateau at conductance i, then number of data points in this bin will be larger than the average for all the traces, $N_i(r) > \langle N_i(r) \rangle$, which gives a positive $\delta N_i(r)$. The same trace has no plateau at any other bin $j(\neq i)$ and so $N_{j(\neq i)}(r) < \langle N_j(r) \rangle$ which gives a negative $\delta N_{j(\neq i)}(r)$ (as long as $\langle N_j(r) \rangle$ exceeds the background). The opposite signs of $\delta N_i(r)$ and $\delta N_{j(\neq i)}(r)$ results in a negative correlation.

In general, conductance plateaus are not exactly flat; they can have a negative slope, due to a decreasing conductance with increasing elongation or in some special cases even show a positive slope, as in Al junctions.[27] The above simulation can be generalized for sloped plateaus (Figure 4d) by considering $\mathscr{G}$ as the random conductance of the *center of the plateau*, distributing the plateau over $2N + 1$ neighbor conductance bins to yield a single-trace conductance histogram of

$$ N_i(r) = \frac{1}{2N+1} \sum_{k=-N..N} \delta_{i,\mathscr{G}(r)+k} + \mathscr{B}(i,r) \quad (9) $$

With this notation the length of the plateaus is still unity, and the plateau center conductance still has a Gaussian distribution (with width $0.06\bar{\mathscr{G}}$). The conductance histogram generated from such simulated traces using $N = 0.06\bar{\mathscr{G}}$, is shown in Figure 4f. This histogram is similar to that generated from traces with flat plateaus (Figure 4c). The corresponding 2DCH in Figure 4e shows a finite width positively correlated region near the diagonal. This is a result of having sloped plateaus since having a plateau at bin i increases the probability of having enhanced conductance counts in bin j when $|i - j| \lesssim N$. In the regions where $|i - j| \gtrsim N$ we see a negative correlation similarly that seen in Figure 4b and for even larger conductance difference an uncorrelated background is observed. This simple example demonstrates how a 2D correlation analysis can distinguish two fundamentally different situations which have nearly identical conductance histograms.

Two Conductance Plateaus. We now turn to the case where there are two plateaus in a trace and study how the relation of these two plateaus can be investigated by correlation analysis. The two bins at which the plateaus are positioned on trace r are determined by two random numbers, $\mathscr{G}_1(r)$ and $\mathscr{G}_2(r)$ which have well separated distributions with mean values of $\bar{\mathscr{G}}_1$ and $\bar{\mathscr{G}}_2$. We use, for this example, uniformly distributed random variables within a width $0.4\bar{\mathscr{G}}_{11}$. The existence of plateaus on a particular trace is determined by two random boolean numbers $\Theta_1(r)$ and $\Theta_2(r)$, which take a
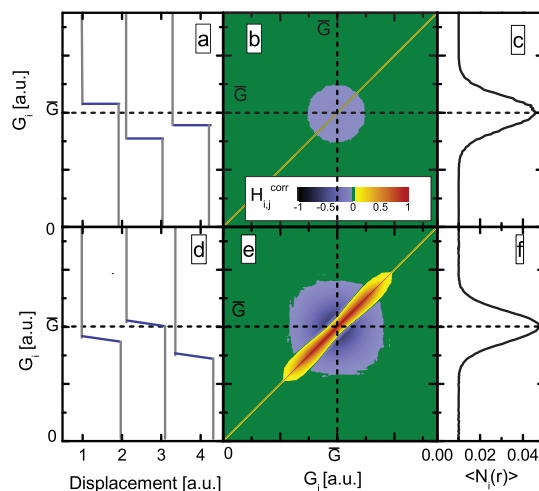

Figure 4. Correlation effects for simulated traces with a single conductance plateau. (a) Conductance traces with flat plateaus. Panels b and c show the 2DCH and the conductance histogram for traces with flat plateaus, respectively. Panels d–f show corresponding figures for traces with a sloped plateau. Although the conductance histogram cannot distinguish flat plateaus from sloped plateaus, this difference is evident in the 2DCH.

value of 1 if a plateau exists and 0 otherwise. Single-trace conductance histograms are generated as

$$ N_i(r) = \Theta_1(r)\delta_{i,\mathscr{G}_1(r)} + \Theta_2(r)\delta_{i,\mathscr{G}_2(r)} + \mathscr{B}(i,r) \quad (10) $$

We first consider a situation in which the two plateaus appear independently from each other; that is, $\Theta_1(r)$ and $\Theta_2(r)$ are independent random variables with a mean value of 0.5. In this case we are equally likely to see traces with (1) two plateaus, (2) a single plateau near $\bar{\mathscr{G}}_1$, (3) a single plateau near $\bar{\mathscr{G}}_2$, or (4) no plateaus, as shown in Figure 5a1. The correlation plot for such simulated traces is shown in Figure 5a2, where we see two square regions around $(i, j) \approx (\bar{\mathscr{G}}_1, \bar{\mathscr{G}}_1)$ and $(\bar{\mathscr{G}}_2, \bar{\mathscr{G}}_2)$ that are negatively correlated and a positively correlated diagonal similar to that in Figure 4b. No *cross correlations* are observed at $(i,j) \approx (\bar{\mathscr{G}}_1, \bar{\mathscr{G}}_2)$. In Figure 5a3, we show the full conductance histogram (shaded gray) and a conditional histogram (orange) created from selected traces that contain plateaus near $\bar{\mathscr{G}}_1$. We see that the conditional histogram peak near $\bar{\mathscr{G}}_1$ is higher than that of the full histogram, but the peak around $\bar{\mathscr{G}}_2$ is the same in both since the plateau occurrence is not correlated.

The example when conductance traces show both plateaus in a correlated manner is shown in Figure 5b. Here, traces either have both plateaus or no plateaus and $\Theta_1(r) = \Theta_2(r)$. The 2DCH (Figure 5b2) shows a clear positive cross correlations (yellow squares) at $(i, j) \approx (\bar{\mathscr{G}}_1, \bar{\mathscr{G}}_2)$. We note here that for a positive cross correlation, it is necessary to have traces when none of the plateaus appear otherwise the cross correlation between the two configurations is zero. Figure 5b3 shows the conditional histogram (orange) of selected traces

that contain a plateau near $\bar{\mathscr{G}}_1$. We see that the peak near $\bar{\mathscr{G}}_2$ is higher in the conditional histogram when compared with that of the full histogram (shaded gray). Again, if all traces had both plateaus, there would be no difference between the conditional histogram and the full histogram.

Figure 5c1 shows traces where the two conductance plateaus are anticorrelated ($\Theta_2(r) = 1 - \Theta_2(r)$) with 50% of the traces having a plateau near $\bar{\mathscr{G}}_1$ and the others having a plateau near $\bar{\mathscr{G}}_2$. The two plateaus never occur in the same trace. The 2DCH generated from these traces (Figure 5c2) shows a clear negative correlation at $(i,j) \approx (\bar{\mathscr{G}}_1, \bar{\mathscr{G}}_2)$. Figure 5c3 shows the conditional histogram (orange) of selected traces that contain a plateau near $\bar{\mathscr{G}}_1$. We see that the peak near $\bar{\mathscr{G}}_2$ is suppressed indicating a negative cross-correlation.

The above cases considered correlations in the *existence* of plateaus. We can also consider cases where both plateaus exist; however, their *length* is anticorrelated. As an example Figure 5d1 demonstrates traces where both plateaus are always observed with the constraint that their length adds up to unity. The resulting 2DCH is very similar to the one shown in Figure 5c2. The conditional histogram can however distinguish these two cases since the peak near $\bar{\mathscr{G}}_2$ is not fully suppressed.

The last case that we consider is when the conductance of the plateaus ($\mathscr{G}_1(r)$ and $\mathscr{G}_2(r)$) are correlated. The simplest example has $\mathscr{G}_2(r) - \mathscr{G}_1(r) = \Delta G$. This implies that the conductance of the first plateau is random, but the conductance of the second plateau is shifted rigidly relative to the conductance of the first plateau (Figure 5e1). In this we still see the regions of negative correlation as above, but in addition, a positive cross correlation is seen if $i - j = \Delta G$ (Figure 5e2). For such traces the second peak of the conditional histogram is unaffected by the selection of traces with plateaus in the first peak region. However, if the selection is not performed for the whole region of the first peak, just for a subset of it, then the corresponding subset of the second peak will be enhanced in the conditional histogram (blue curve).

These five examples detailed above demonstrate how a correlation analysis can be used to obtain new information on the occurrence and length of conductance plateaus. These basic types of correlations correspond to fundamentally different relations between two hypothetic junction configurations, which cannot be resolved by the conductance histogram.

Multiple Conductance Plateaus. Finally, we consider two simple models for traces with multiple conductance plateaus. In the first model five plateaus are considered at five independent uniformly distributed conductances values $\mathscr{G}_i$ within the conductance interval of $0-8$. To mimic a finite jump between adjacent plateaus only those sets of random numbers are used,
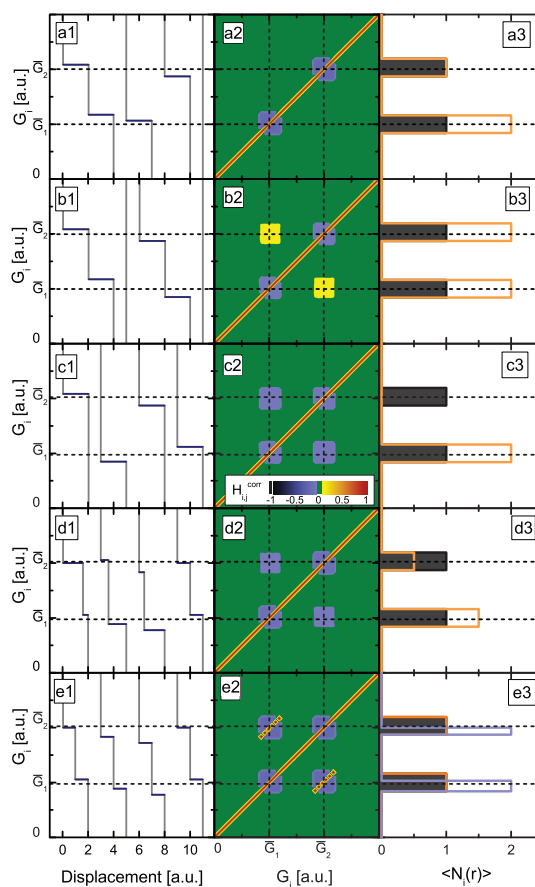

Figure 5. Correlation effects for simulated traces with two conductance plateaus. The left panels show different types of traces, the middle panels show the corresponding simulated 2DCH and the right panels show conductance (gray) and conditional histograms (orange, blue) as discussed in the text. Panel a represents traces where the occurrence of the two plateaus is independent. Panels b and c have traces where the two plateaus appear together (b) or exclude each other (c). Panels d and e have traces with both plateaus exhibiting anticorrelation in the length (d) or correlation in the conductance (e). All the panels correspond to 20 000 simulated traces.

for which $|\mathscr{G}_i - \mathscr{G}_j| > \Delta G_{jump}$ for any i,j pair, where $\Delta G_{jump} = 0.5$ defines the minimal amplitude of the conductance jumps. Furthermore, plateaus with finite slope are considered similar to eq 9 (Figure 6a). This model produces the correlation plot shown in Figure 6b. We see a finite width positively correlated region around the diagonal. The width of this region along the horizontal (or vertical) direction describes the average width of the plateaus along the conductance axis, $\Delta G_{plateau}$ (0.25 used here). Away from the diagonal a negatively correlated *stripe* is observed, which has a width that corresponds to the conductance jumps between plateaus. Beyond this region, no correlation is seen since for large conductance differences, a plateau can be followed either by a conductance jump or another plateau.

In the second model, we consider traces where adjacent plateaus are separated by a well-defined

conductance value. We use traces with five sloped plateaus ($\Delta G_{plateau} = 0.5$) within the interval of 0−8. The conductance of the last plateau ($\mathscr{G}_1$) is a random variable with a Gaussian distribution ($\bar{\mathscr{G}}_1 = 2$ and $\sigma = 0.12$). All other plateaus are obtained by requiring that $\mathscr{G}_i = (i − 1) + \mathscr{G}_1$, as shown in Figure 6d. For such traces the histogram (Figure 6f) shows no clear peaks; however, the correlation plot shows stripes (Figure 6e). The distance of the positively correlated stripes along the horizontal (or vertical) axis corresponds to the well-defined separation of neighbor plateau conductances.

Correlation Analysis of Experimental Data. To demonstrate the application of correlation analysis to experimentally measured conductance traces, we construct and analyze the 2DCHs of four different metal nanoscale contacts including Al, Ta, Fe, and V, and single-molecule junctions created using CO and 4,4′-bipyridine.

Aluminum Junctions—The Internal Structure of a Histogram Peak. Conductance histograms and 2DCH plots for break-junction measurements with Al were introduced in Figure 1c and Figure 3d to demonstrate the analysis technique. The conductance histogram for Al junctions exhibit several peaks, with the lowest one at $G \approx 0.7$ G_0, attributed to a single-atom contact,[1,28] which is probably a dimer configuration.[29,30] In general, this lowest conductance peak does not exhibit any internal structure, however, the 2DCH (Figure 3d) shows rich structure in the conductance region spanned by this peak, which we will discuss in detail further below. At higher conductances the 2DCH (Figure 3d) is very similar to that of the simulated one (Figure 6b) where we considered a random series of sloped conductance plateaus in the individual traces. We see a finite width positively correlated region around the diagonal, which reflects the presence of plateaus with finite slope. Beyond this region, a negatively correlated stripe is observed indicating that the sloped plateaus are separated by finite jumps in conductance. There are no other correlations detected beyond this region.

The 2DCH around the region of the first histogram peak can be separated into three different regions as delineated by the white lines in Figure 3d and by colored regions in the conductance histogram. The first region (orange) which spans $G \approx 0.15−0.6$ G_0 shows a broad positively correlated area around the diagonal. The second region (yellow) which spans $G \approx 0.6−1$ G_0 shows a narrow positively correlated region around the diagonal and a broader negatively correlated region beyond the diagonal. The negative correlation at the intersection with the first region implies that if a trace has a conductance plateau in this second region, then it is unlikely to have another plateau in the first conductance region. The third region (red) spanning $G \approx 1−1.4$ G_0 has a clear positively correlated region where it intersects the first region, away from
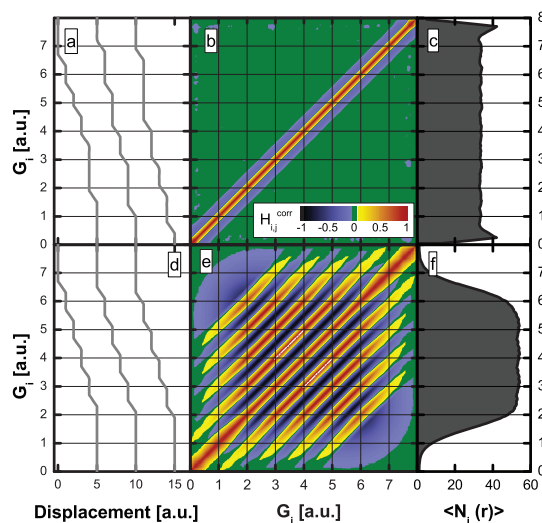

Figure 6. Correlation effects for simulated traces with multiple conductance plateaus. Panels a, b, and c demonstrate example traces, the 2DCH and the conductance histogram for simulated traces with five random plateau conductances and a finite minimal amplitude of the conductance jump between neighbor plateaus. Panels d, e, and f demonstrate example traces, the 2DCH, and the conductance histogram for traces with five plateaus separated by a fixed conductance difference.

the diagonal, whereas it is negatively correlated with the second region. Thus traces that have a final plateau around $G \approx 0.15−0.6$ G_0 are likely to result from junctions with a conductance around $G \approx 1−1.4$ G_0, whereas a plateau in the second region is usually not preceded by another one in the third region. The second region does not show a positive correlation with higher conductance intervals. This implies that no typical configuration is identified prior to a plateau in the second region. The clear difference in correlation between traces that have conductance plateaus in the first or second conductance region indicates the presence of two fundamentally different Al single-atom contacts even though they contribute to the same peak in the conductance histogram.

The rich structure of the correlation plot in the region of the first histogram peak has inspired us to study Al junctions in more detail, investigating numerous sample wires. We have found that in some devices (<5% of all devices studied) the conductance histogram shows a split first peak (Figure 7a). In such cases, the conductance histogram can distinguish the two configurations which are otherwise only seen in the 2DCH analysis. The 2DCH generated from this data set is shown in Figure 7b, and generally exhibits the same features as the one in Figure 3d. The split first peak however, allows us to study conditional histograms created from traces that have a plateau either in the first region (orange) or the second (yellow).

The conditional histograms from traces that contribute to the first (second) subpeak are shown in blue (green) in Figure 7a. We see that selecting traces that

contribute to the first (second) subpeak results in a suppression of the second (first) subpeak. This complete suppression of the conditional histogram peaks points to a strong anticorrelation in the existence of the two distinct configurations, similarly to results from simulated traces shown in Figure 5c3. These conditional histograms also show that the peak heights are different. Since these histograms are normalized by the number of traces, this height difference indicates that plateaus that contribute to the lower conductance peak are on average longer than those that contribute to the second subpeak as shown in the sample traces in Figure 7c.

These data indicated that there are two structurally different final junction configurations in Al point-contacts which do not occur in the same traces. We also see, from the 2DCH, that traces that have a plateau in the orange conductance region are also likely to have a plateau in the red conductance region as demonstrated in the sample traces (Figure 7c). These two distinct final junction configurations may be related to two structurally different single atom contacts, although the details of these structures can only be determined from detailed theoretical models.

Tantalum Junctions—Presence and Absence of Adhesive Instabilities. As a next example we discuss results from break-junction measurements of Ta junctions. Ta is a *d*-metal with 4−5 open conductance channels for a single atom contact.[31] In *d*-metals the transport through highly oriented *d* orbitals is expected to be extremely sensitive to the precise atomic geometry of the junction.[32] Due to this sensitivity to contact structure, junctions with the same number of atoms in the smallest cross section may show a broad range of conductance. This leads to conductance histograms having few clear peaks. Indeed, in Ta the first histogram peak, which is attributed to single atom contacts, is rather broad, and no further peaks are seen at higher conductances (Figure 8a). In addition, the histogram shows a large number of counts at low conductances $G < 1\ G_0$ due to tunneling conductance between the broken contacts.

The 2D correlation histogram (Figure 8b) shows strong anticorrelation between the peak region (yellow region in Figure 8a) and the low-conductance tail region (orange region in Figure 8a). This is also demonstrated by the conditional histograms in Figure 8a generated from selected traces that contribute to the first conductance peak or the tail conductance region. Thus traces that have a long plateau at the first conductance peak are unlikely to have large weight in the tail region, while traces that have a short plateau corresponding to the single-atom contact show a large number of counts below this conductance. Furthermore, the 2DCH exhibits a broad positively correlated spot where the tail region intersects with itself which indicates that counts in
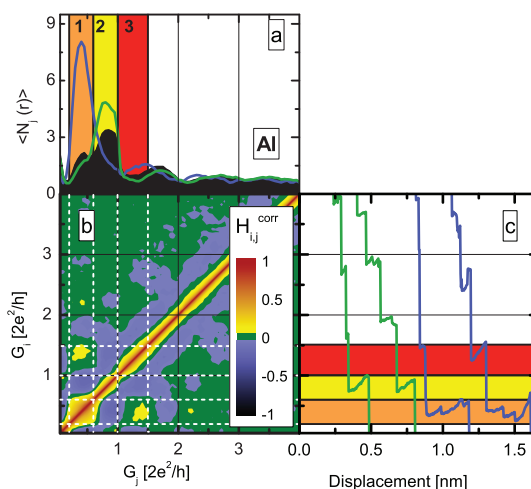

Figure 7. Al break-junction measurements for a data set showing a clear split in first histogram peak. (a) Conductance histogram (shaded black) and two conditional histograms (blue and green) as detailed in the text. (b) 2DCH and (c) sample conductance traces chosen from the data set of the blue and green conditional histograms. The three conductance regions denoted by different colors in panels a and c are projected to the 2DCH by white dashed lines.

this tail region result from highly sloped features in individual conductance traces, indicative of a tunneling.

These features indicate that a Ta contact can rupture in two different ways: (i) the single-atom contact can be stretched during the elongation resulting in a long plateau and then rupture to a broken junction where the apex of the electrodes are far apart, resulting in a small contribution to the tunneling conductance (few counts in the tail region). Such examples are illustrated by green example traces in Figure 8c. (ii) A short single-atom plateau is followed by a continuous decay of the conductance in the tail region (blue traces in Figure 8c). The former type of junction evolution, which occurs in most metals, is known as adhesive instability of the junction,[24] where a large gap is opened up between the broken electrodes after the rupture of the single-atom contact. The occasional absence of the adhesive instability which is resolved by the 2DCH of Ta, was indeed reported in Ta, Mb, and W point-contacts.[33]

Iron and Vanadium Junctions—Correlated Shifting of Plateaus. For the Al and Ta measurements, the correlation plot does not show any special features at high conductances corresponding to junctions with more than one atom in the minimal cross section. In the following we show a different behavior for Fe and V contacts, which are similar what was studied in detail in Ni break-junction measurements in ref 13. Conductance histograms and 2DCHs for break-junction measurements of Fe[34,35] and V junctions are shown in Figure 9. Both conductance histograms (shaded black) show a single pronounced peak at $G \approx 2\ G_0$ and no features at conductances greater than 5 G_0. In contrast

the 2DCH exhibits clearly resolved stripes up to much higher conductance values that resemble the simulated 2DCHs shown in Figure 6e. These stripes demonstrate that the conductance traces show a very regular pattern even at rather high conductance values with a well-defined conductance difference between successive plateaus. However, the absolute conductance of the plateaus changes from trace to trace, which causes the smearing of the conductance histogram. This regular pattern is also resolved by conditional histograms, as demonstrated by the blue (green) curves in Figure 9a,b showing $H_{i,j}^{cond}$ with $G_j = 11\ G_0$ ($G_j = 12\ G_0$). These curves demonstrate that once the initial conductance is fixed, a well-defined sequence of plateau conductances is resolved.

This correlated shifting of the plateaus may have different origins, including a change of the contact geometry (*e.g.*, the crystallographic orientation) from junction to junction, or the presence of some defects pinned to the vicinity of the contact. The observed stripe structure points to a very regular narrowing of the junction, with a well-defined amplitude of the conductance jumps, which is in contrast to the majority of the metals where the amplitude of the conductance jump can be stochastic. The observation of stripes in the 2DCH opens a new window to resolve the details of junction formation dynamics, despite having no clear structures in the conductance histogram.

Platinum−Carbon Monoxide−Platinum Single-Molecule Junctions−Correlations Between Molecular Configurations. In the following we show an example for the correlation analysis of single molecule Pt−CO−Pt junctions. Figure 10a shows a conductance histogram of Pt point-contacts measured in an environment of CO. Beside the characteristic single-atom contact peak at 2 G_0, two additional peaks are seen at 0.5 G_0 and $G \approx 1$ G_0.[36,37] Theoretical simulations have shown that the 0.5 G_0 conductance feature corresponds to junction where the Pt contacts are bridged with a CO molecule that is aligned with the contact axis, while the $\sim$1 G_0 junction presumably has the CO molecule oriented perpendicular to the contact axis.[38]

In Figure 10b, we show the 2DCH constructed from this data, where we see that the two junctions (with conductance around 0.5 G_0 and 1 G_0) occur in an uncorrelated manner; that is, these are two independent molecular configurations. This means that the formation of one molecular configuration neither helps nor hampers the formation of the other configuration. In contrast both molecular configurations are anticorrelated with the configuration attributed to the single-atom contacts ($\sim$2 G_0). In the conditional histograms the selection for either of the molecular configurations only reduces the amplitude of the pure Pt peak, which may point to the anticorrelation in the plateau lengths.
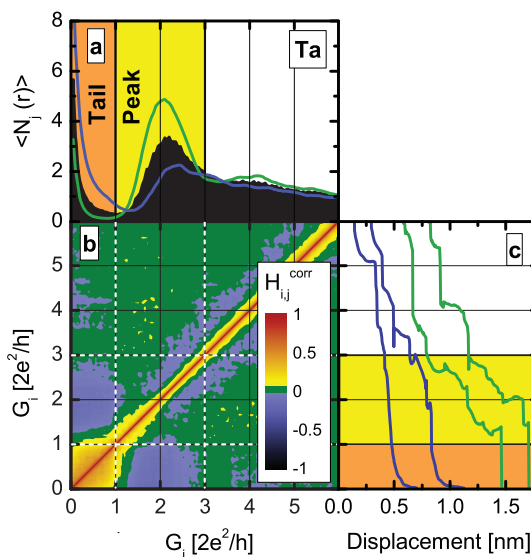

Figure 8. Ta break-junction measurements. (a) Conductance histogram (shaded black) and two conditional histograms (blue and green) constructed for the orange and yellow conductance region, respectively. (b) 2DCH and (c) sample conductance traces chosen from the data set of the blue and green conditional histograms. The two conductance regions denoted by different colors in panels a and c are projected to the 2DCH by white dashed lines.

The correlation analysis can be interpreted as follows. In some traces, we do not see a molecular plateau, just a Pt single-atom contact signature, as demonstrated by the first example trace in Figure 10c. In other traces, when a molecule is incorporated in the Pt atomic junction, the single-atom contact plateau is generally shorter. Finally, the negligible correlation between the perpendicular and the parallel configuration means that these two configurations can occur in the same trace (though not in every trace.) This demonstrates that the correlation analysis can be applied as a powerful tool to determine how the formation of one molecular configuration influences the formation of another.

Au−4,4′-Bipyridine−Au Single Molecule Junctions— Switching between Distinct Binding Configurations. In our final example, we demonstrate the application of correlation analysis on single Au−4,4′-bipyridine−Au molecular junctions. It has been shown that these molecular junctions form two stable configurations with different well-separated conductances.[11] Since the conductance of these molecular junctions is several orders of magnitude smaller than that of the Au point-contact, conductance histograms and 2DCH plots are investigated using a logarithmic conductance scale.[8] Figure 11a shows the conductance histogram (shaded black) where two molecular peaks are clearly visible. These span the conductance regions $G \approx 2 \times 10^{-4}\ G_0$ (low G) and $G \approx 1 \times 10^{-3}\ G_0$ (high-G), as shown by the orange and yellow shading. The characteristic peak of a pure gold junction at $G = 1\ G_0$ is also seen. This histogram was generated from 10 000 conductance traces measured
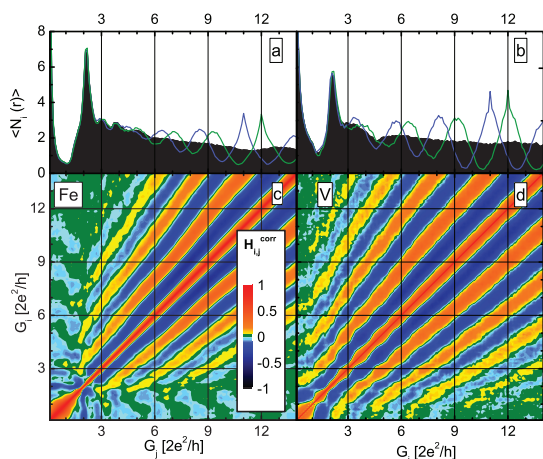
Figure 9. Panels (a,c) and (b,d) show conductance histograms (shaded black) and the 2DCHs for Fe and V junctions, respectively. The green and blue lines in panels a and b show conditional histograms as defined in the text.

in a scanning tunneling microscope based break-junction set up under ambient conditions as detailed in ref 11. These two configurations result from two types of binding geometries (Figure 11b): the conductance is low if the molecule bridges the apex of both Au electrodes in a vertical geometry and high when the geometry permits an additional π-coupling between the pyridine ring and electrodes. The high-G configuration is seen when the separation between the electrodes is smaller than the length of the molecule. It was found that the molecular junction could be switched reversibly between these two configurations by compressing and elongating the junction.[11]

The presence of two distinct molecular configurations with distinct conductance makes this system an ideal one for a correlation analysis. Figure 11c shows the 2DCH generated from all traces excluding a few (<1%) that do not break from a 1 G_0 contact to an open junction within a 1 nm displacement (comparable to the length of the molecule). The correlation plot shows rich structures; here, we focus on the relation of the two molecular configurations. We see a clear blue negatively correlated region where the high-G and low-G ranges cross. To determine if this results from an anticorrelation in the existence of both plateaus or in the length of the plateaus, we also create conditional histograms (Figure 11a) by selecting traces that contribute to the high-G peak (blue region) or low-G peak (green region). We see that these conditional histograms still show both peaks, indicating that neither plateau is completely suppressed in the selected subsets. The conditional histogram created from traces with a long high-G plateau shows only a suppression of the upper part of the low-G peak ($G \approx 1.8 \times 10^{-4} - 3.1 \times 10^{-4}$ G_0). Similarly, the histogram from traces containing a long plateau in the low-G region show a suppression of part of the high-G peak ($G \approx 3.1 \times 10^{-4} - 1.3 \times 10^{-3}$ G_0). This observed negative
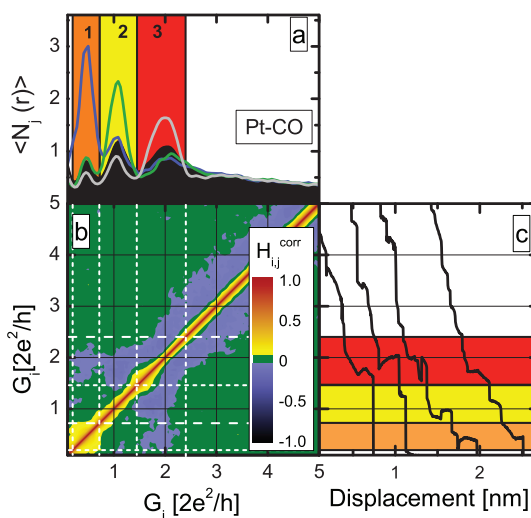

Figure 10. Pt break-junction measurements in an CO environment. (a) Conductance histogram (shaded black) and three conditional histograms (blue, green, and gray) constructed for the orange, yellow, and red conductance regions, respectively. (b) 2DCH and (c) sample conductance traces chosen from the whole data set. The three conductance regions denoted by different colors in panels a and c are projected to the 2DCH by white dashed lines.
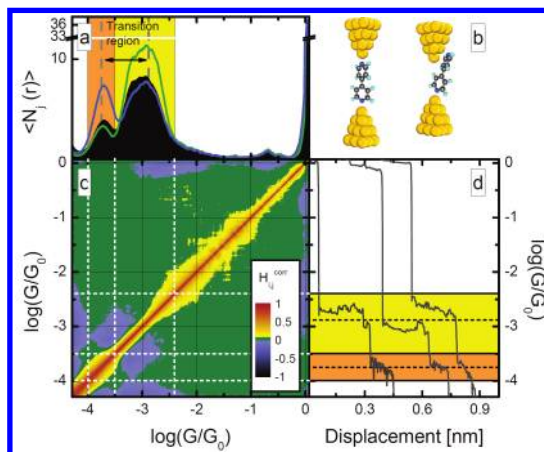

Figure 11. Correlation analysis of Au—4,4′-bipyridine—Au junctions. (a) Conductance histogram using equidistant bins at the logarithmic conductance scale (shaded black). The green (blue) lines show the conditional histograms constructed for the high-G (low-G) interval as a reference region. The dashed lines demonstrate the borders of the transition region, where the conditional histograms deviate from the total histogram. (b) Two binding configurations of Au—4.4′-bipyridine—Au single-molecule junctions. (c) 2DCH using equidistant bins at the logarithmic conductance scale. (d) Sample conductance traces. The dashed lines demonstrate the borders of the transition region.

correlation is therefore not an anticorrelation in the existence of the two configurations as is demonstrated by the conditional histogram, but an anticorrelation in the length of the plateaus as illustrated in Figure 5d.

The structure of the conditional histograms provide new insight into these junction elongation trajectories. In both the high-G and low-G region the conductance is decreasing during the elongation of the junction.

The transition between the two configurations is reflected by a sudden jump, but this jump is not always situated at exactly the same conductance, its position can vary within a transition interval. If the jump starts at higher (lower) conductance then the high-G plateau will be shorter (longer) than average. The opposite will be true of the low-G plateau resulting in the observed negative correlation. Outside of this transition region no correlations are detected. In this sense the conditional histograms can be used to identify the statistically relevant transition region between the two configurations: according to Figure 11a the transition occurs in the conductance interval of $\sim 1.8 \times 10^{-4}$ to 1.3×10^{-3} G_0, where the conditional histograms show negative deviation from the total histogram. (Note, that the conditional histograms should only be studied in the region outside of the reference interval, the increase of the peak in the reference interval is an obvious result of the selection.) The above interpretation is demonstrated by the example traces in Figure 11d, where the amplitude of the conductance jump is always similar, but its position varies in the transition region.

CONCLUSIONS

Break junction techniques have proven to be powerful for characterizing electronic properties of single-atom and single molecule junctions. This method provides the possibility to investigate a large statistical ensemble of independently created nanoscale junctions which have inherently stochastic formation dynamics. Conductance histograms, which are widely used to analyze such data, provide only a basic analysis method. Here, we have shown that additional information can be obtained about nanoscale junctions by creating and analyzing two-dimensional correlations histograms (2DCH).

We first illustrate different features that can be seen in 2DCH using simulated conductance traces. We use this to show that for systems having two different junction configurations, the 2DCH can be used to distinguish cases where the configurations occur in a correlated, anticorrelated, or uncorrelated manner. We then apply this analysis technique to two different classes of nanoscale junctions; metal point-contacts including Al, Ta, Fe, and V junctions and single molecule junctions including Pt—CO—Pt and Au—4,4′-bipyridine—Au junctions. Our results from the analysis of these data demonstrate that a correlation analysis can provide additional information about the formation and evolution of nanoscale junctions beyond what can be determined from conductance histograms alone. With the development of simulation techniques[39] a correlation analysis may also be used to compare experiments with simulated conductance traces, going beyond the comparison of a histogram peak position with a single calculated conductance value. The correlation analysis also provides complementary information to 2D conductance-displacement histograms discussed here, and the combination of these two methods can bring essential information to the understanding of atomic and single-molecule structures solely by a progressive analysis of the conductance traces.

REFERENCES AND NOTES

1. Agrat, N.; Levy Yeyati, A.; van Ruitenbeek, J. M. Quantum Properties of Atomic-Sized Conductors. *Phys. Rep.* **2003**, *377*, 81–279.

2. Cuevas, J. C.; Scheer, E. *Molecular Electronics An introduction to Theory and Experiment*; World Scientific: Singapore, 2010.

3. Li, C.; Pobelov, I.; Wandlowski, T.; Bagrets, A.; Arnold, A.; Evers, F. Charge Transport in Single Au|Alkanedithiol|Au Junctions: Coordination Geometries and Conformational Degrees of Freedom. *J. Am. Chem. Soc.* **2008**, *130*, 318–326.

4. Venkataraman, L.; Klare, J. E.; Tam, I. W.; Nuckolls, C.; Hybertsen, M. S.; Steigerwald, M. L. Single-Molecule Circuits with Well-Defined Molecular Conductance. *Nano Lett.* **2006**, *6*, 458–462.

5. Reed, M. A.; Zhou, C.; Muller, C. J.; Burgin, T. P.; Tour, J. M. Conductance of a Molecular Junction. *Science* **1997**, *278*, 252–254.

6. Smit, R. H. M.; Noat, Y.; Untiedt, C.; Lang, N. D.; van Hemert, M. C.; van Ruitenbeek, J. M. Measurement of the Conductance of a Hydrogen Molecule. *Nature* **2002**, *419*, 906–909.

7. Xu, B.; Tao, N. J. Measurement of Single-Molecule Resistance by Repeated Formation of Molecular Junctions. *Science* **2003**, *301*, 1221–1223.

8. González, M. T.; Wu, S.; Huber, R.; van der Molen, S. J.; Schönenberger, C.; Calame, M. Electrical Conductance of Molecular Junctions by a Robust Statistical Analysis. *Nano Lett.* **2006**, *6*, 2238–2242.

9. Yanson, A. I.; Rubio Bollinger, G.; van den Brom, H. E.; Agraït, N.; van Ruitenbeek, J. M. Formation and Manipulation of a Metallic Wire of Single Gold Atoms. *Nature* **1998**, *395*, 783–785.

10. Smit, R. H. M.; Untiedt, C.; Yanson, A. I.; van Ruitenbeek, J. M. Common Origin for Surface Reconstruction and the

Formation of Chains of Metal Atoms. *Phys. Rev. Lett.* **2001**, *87*, 266102.

11. Quek, S. Y.; Kamenetska, M.; Steigerwald, M. L.; Choi, H. J.; Louie, S. G.; Hybertsen, M. S.; Neaton, B. J.; Venkataraman, L. Mechanically Controlled Binary Conductance Switching of a Single-Molecule Junction. *Nat. Nanotechnol.* **2009**, *4*, 230–234.

12. Martin, C. A.; Ding, D.; Sörensen, J. K.; Björnholm, T.; van Ruitenbeek, J. M.; van der Zant, H. S. J. Fullerene-Based Anchoring Groups for Molecular Electronics. *J. Am. Chem. Soc.* **2008**, *130*, 13198–13199.

13. Halbritter, A.; Makk, P.; Mackowiak, S.; Csonka, S.; Wawrzyniak, M.; Martinek, J. Atomic Narrowing of Ni, Fe, and V Nanowires Resolved by Two-Dimensional Correlation Analysis. *Phys. Rev. Lett.* **2010**, *105*, 266805.

14. González, M. T.; Leary, E.; García, R.; Verma, P.; Herranz, M. Á.; Rubio-Bollinger, G.; Martín, N.; Agraït, N. Break-Junction Experiments on Acetyl-Protected Conjugated Dithiols under Different Environmental Conditions. *J. Phys. Chem. C.* **2011**, *115*, 17973–17978.

15. Tam, E. S.; Parks, J. J.; Shum, W. W.; Zhong, Y.-W.; Santiago-Berriíos, M. B.; Zheng, X.; Yang, W.; Chan, G. K.-L.; Abruna, H. D.; Ralph, D. C. Single-Molecule Conductance of Pyridine-Terminated Dithienylethene Switch Molecules. *ACS Nano* **2011**, *5*, 5115–5123.

16. Mishchenko, A.; Zotti, L. A.; Vonlanthen, D.; Bürkle, M.; Pauly, F.; Cuevas, J. C.; Mayor, M.; Wandlowski, T. Single-Molecule Junctions Based on Nitrile-Terminated Biphenyls: A Promising New Anchoring Group. *J. Am. Chem. Soc.* **2011**, *133*, 184–187.

17. Wawrzyniak, M.; Martinek, J.; Susla, B.; Ilnicki, G. Correlation Histograms in Conductance Measurements of Nanowires Formed at Semiconductor Interfaces. *Acta Phys. Pol., A* **2009**, *115*, 384–386.

18. Ernst, R. R.; Bodenhausen, G.; Wokaun, A. *Principles of Nuclear Magnetic Resonance in One and Two Dimensions*; Oxford Univ. Press: Oxford, UK, 1987.

19. Nazarov, Y. V., Ed. *Quantum Noise in Mesoscopic Physics*; Kluwer: Dordrecht, The Netherlands, 2003.

20. Brown, R. H.; Twiss, R. Q. Correlation between Photons in two Coherent Beams of Light. *Nature* **1956**, *177*, 27–29.

21. Henny, M.; Oberholzer, S.; Strunk, C.; Heinzel, T.; Ensslin, K.; Holland, M.; Schönenberger, C. The Fermionic Hanbury Brown and Twiss Experiment. *Science* **1999**, *284*, 296–298.

22. Oliver, W. D.; Kim, J.; Liu, R. C.; Yamamoto, Y. Hanbury Brown and Twiss-Type Experiment with Electrons. *Science* **1999**, *284*, 299–301.

23. Burkard, G.; Loss, D.; Sukhorukov, E. V. Noise of Entangled Electrons: Bunching and Antibunching. *Phys. Rev. B* **2000**, *61*, R16303–R16306.

24. Trouwborst, M. L.; Huisman, E. H.; Bakker, F. L.; van der Molen, S. J.; van Wees, B. J. Single Atom Adhesion in Optimized Gold Nanojunctions. *Phys. Rev. Lett.* **2008**, *100*, 175502.

25. Csonka, S.; Halbritter, A.; Mihály, G. Pulling Gold Nanowires with a Hydrogen Clamp: Strong Interactions of Hydrogen Molecules with Gold Nanojunctions. *Phys. Rev. B* **2006**, *73*, 075405.

26. Halbritter, A.; Csonka, S.; Mihály, G.; Shklyarevskii, O. I.; Speller, S.; van Kempen, H. Quantum Interference Structures in the Conductance Plateaus of Gold Nanojunctions. *Phys. Rev. B* **2004**, *69*, 121411.

27. Cuevas, J. C.; Levy Yeyati, A.; Martn-Rodero, A.; Rubio Bollinger, G.; Untiedt, C.; Agrat, N. Evolution of Conducting Channels in Metallic Atomic Contacts Under Elastic Deformation. *Phys. Rev. Lett.* **1998**, *81*, 2990–2993.

28. Scheer, E.; Agraït, N.; Cuevas, J. C.; Levy Yeyati, A.; Ludoph, B.; Martín-Rodero, A.; Rubio Bollinger, G.; van Ruitenbeek, J. M.; Urbina, C. The Signature of Chemical Valence in the Electrical Conduction through a Single-Atom Contact. *Nature* **1998**, *394*, 154–157.

29. Jelínek, P.; Perez, R.; Ortega, J.; Flores-F, F. First-Principles Simulations of the Stretching and Final Breaking of Al Nanowires: Mechanical Properties and Electrical Conductance. *Phys. Rev. B* **2003**, *68*, 085403.

30. Hasmy, A.; Pérez-Jiménez, A. J.; Palacios, J. J.; García-Mochales, P.; Costa-Krämer, J. L.; Díaz, M.; Medina, E.; Serena, P. A. Ballistic Resistivity in Aluminum Nanocontacts. *Phys. Rev. B* **2005**, *72*, 245405.

31. Makk, P.; Csonka, S.; Halbritter, A. Effect of Hydrogen Molecules on the Electronic Transport Through Atomic-Sized Metallic Junctions in the Superconducting State. *Phys. Rev. B* **2008**, *78*, 045414.

32. Pauly, F.; Dreher, M.; Viljas, J. K.; Häfner, M.; Cuevas, J. C.; Nielaba, P. Theoretical Analysis of the Conductance Histograms and Structural Properties of Ag, Pt, and Ni Nanocontacts. *Phys. Rev. B* **2006**, *74*, 235106.

33. Halbritter, A.; Csonka, S.; Mihály, G.; Jurdik, E.; Kolesnychenko, O. Y.; Shklyarevskii, O. I.; Speller, S.; van Kempen, H. Transition from Tunneling to Direct Contact in Tungsten Nanojunctions. *Phys. Rev. B* **2003**, *68*, 035417.

34. Untiedt, C.; Dekker, D. M. T.; Djukic, D.; van Ruitenbeek, J. M. Absence of Magnetically Induced Fractional Quantization in Atomic Contacts. *Phys. Rev. B* **2004**, *69*, 081401(R).

35. Calvo, M. R.; Fernandez-Rossier, J.; Palacios, J. J.; Jacob, D.; Natelson, D.; Untiedt, C. The Kondo Effect in Ferromagnetic Atomic Contacts. *Nature* **2009**, *458*, 1150–1153.

36. Tal, O.; Kiguchi, M.; Thijssen, W. H. A.; Djukic, D.; Untiedt, C.; Smit, R. H. M.; van Ruitenbeek, J. M. Molecular Signature of Highly Conductive Metal−Molecule−Metal Junctions. *Phys. Rev. B* **2009**, *80*, 085427.

37. Kiguchi, M.; Djukic, D.; van Ruitenbeek, J. M. The effect of bonding of a CO molecule on the conductance of atomic metal wires. *Nanotechnology* **2007**, *18*, 035205.

38. Strange, M.; Thygesen, K. S.; Jacobsen, K. W. Electron Transport in a Pt−CO−Pt Nanocontact: Density Functional Theory Calculations. *Phys. Rev. B* **2006**, *73*, 125424.

39. Makk, P.; Visontai, D.; Oroszlány, L.; Manrique, D. Z.; Csonka, S.; Cserti, J.; C., L.; Halbritter, A. Advanced Simulation of Conductance Histograms Validated through Channel-Sensitive Experiments on Indium Nanojunctions. *Phys. Rev. Lett.* **2011**, *107*, 276801.